INTER-AMERICAN TROPICAL TUNA COMMISSION

SCIENTIFIC ADVISORY COMMITTEE

17TH MEETING

La Jolla, California (USA)
8-12 June 2026

DOCUMENT SAC-17-03

STOCK ASSESSMENT OF BIGEYE TUNA IN THE EASTERN PACIFIC OCEAN: 2026 UPDATE ASSESSMENT

Haikun Xu

SUMMARY

1. The 2024 benchmark assessment of bigeye tuna in the eastern Pacific Ocean continues to use a risk analysis approach to provide management advice. The risk analysis encompasses three hierarchically structured levels of hypotheses designed to address the principal sources of uncertainty in the assessment: (1) the misfit to the length composition data for the longline fishery that is assumed to have an asymptotic selectivity; (2) the degree of effort creep (increase in catchability) in the longline fishery; and (3) the steepness of the stock-recruitment relationship.
2. This benchmark assessment was updated in 2026 with two additional years (2024 and 2025) of catch data, longline index of relative abundance, and length composition data. No other modifications were made for this update assessment.
3. Four models (the initial reference model, estimating growth, dome-shaped selectivity for all fisheries, and estimating natural mortality) are considered for the first-level hypothesis, three rates of annual increase in longline catchability (0%, 1%, and 2%) are considered for the second-level hypothesis, and three values of steepness (1.0, 0.9, and 0.8) are considered for the third-level hypothesis. The combination of the three levels of hypotheses results in thirty-six reference models, all of which achieved convergence with positive-definite Hessians in this update assessment.
4. The 2024 benchmark assessment indicated that fishing mortality decreased significantly in 2022-2023 after the introduction of individual vessel threshold (IVT) measure that reduced purse-seine catches of juvenile bigeye tuna.
5. This update assessment indicated that fishing mortality continued to decrease in 2024 and 2025, reaching the lowest levels since 2000.
6. This update assessment also suggests that spawning biomass increased in 2025, as confirmed by the longline index of abundance, which corresponds to decreased fishing mortality in the early 2020s.
7. The overall results (joint probability distributions) of the risk analysis, summarized across the thirty-six reference models, indicate the following:
   a. **19.5%** probability that the spawning biomass at the beginning of 2026 falls below the target reference point associated with the MSY (median $S_{current}/S_{MSY\_d} = 1.43$).
   b. **0.3%** probability that the average fishing mortality in 2023-2025 exceeds the target reference

point associated with the MSY (median $F/F_{MSY} = 0.52$).

c. **53.4%** probability that the spawning biomass at the beginning of 2026 falls below the target reference point associated with 30% dynamic SBR (median $S/S_{30\%} = 0.98$).
d. **3.0%** probability that the average fishing mortality in 2023-2025 exceeds the alternative target reference point associated with 30% dynamic SBR (median $F/F_{30\%} = 0.70$).
e. **0.0%** probability that the spawning biomass at the beginning of 2026 falls below the limit reference point associated with 7.7% SBR (median $S/S_{limit} = 3.45$).
f. **0.0%** probability that the average fishing mortality in 2023-2025 exceeds the limit reference point associated with 7.7% SBR (median $F/F_{limit} = 0.33$).

1. INTRODUCTION

The most recent benchmark assessment for bigeye tuna in the eastern Pacific Ocean (EPO) was conducted in 2024 (SAC-15-02). This report presents the results of the 2026 update assessment for bigeye tuna in the EPO. Data updated for this assessment include new longline indices of relative abundance, longline and purse-seine catches, and purse-seine length compositions for 2024 and 2025, new longline length compositions for 2023 and 2024, and updated data for previous years were available, all of which were incorporated to estimate the current stock status. All model assumptions and parameters in this update assessment are set identically to those employed in the 2024 benchmark assessment.

2. DATA

2.1. Fishery definitions

Twenty-two fishery fleets are defined for bigeye tuna in this update assessment, classified by gear type (purse-seine or longline), purse-seine set type (floating-object (OBJ) or unassociated (NOA)), area of operation (Figure 1), and unit of longline catch (numbers or weight) (Table 1). Due to insufficient length composition data and a negligible contribution to total bigeye catch, both pole-and-line and dolphin-associated purse-seine catches are pooled into the NOA fisheries in this update assessment. The twenty-two fishery fleets comprise fourteen longline fishery fleets, five OBJ fishery fleets, one OBJ discard fleet, and two NOA fishery fleets. The aggregated length frequencies of bigeye tuna exhibit a single mode for most fisheries (Figure 2), suggesting that the majority of fisheries defined by the regression tree analysis contain consistent fishing approaches, and that the double-normal curve is therefore appropriate for estimating selectivity.

2.2. Catch

Catch data for both longline and purse-seine fisheries have been updated up to the final quarter of 2025. Annual bigeye catch from the purse-seine fishery has declined substantially since the implementation of the individual vessel threshold (IVT) measure to reduce bigeye catches in 2022, with values for both 2024 and 2025 approximating 40,000 mt (Figure 3). Annual bigeye catch from the longline fishery has remained stable at approximately 28,000 mt since the introduction of the IVT in 2022. The recorded values for 2024 and 2025 are 27,000 mt and 20,000 mt, respectively; the latter figure is likely under-estimated owing to delayed data reporting characteristic of the longline fishery.

2.3. Index of relative abundance

Indices of relative abundance are a critical input to stock assessment models as they directly inform how population abundance changes over time. Although both purse-seine and longline indices of abundance are available for bigeye in the EPO, this assessment incorporates only the longline index, which primarily reflects the abundance of mature bigeye. The index fleet is based on fishery-dependent catch-per-unit-effort (CPUE) data collected by the Japanese longline fleet that persistently targets bigeye tuna in the EPO.

Both fishing effort and spatial coverage of the Japanese longline fleet operating in the EPO have declined approximately linearly since around 1993 (Figure 4).

The longline index of abundance for bigeye tuna in the EPO has been updated using the same standardization methodology as that applied in the most recent benchmark assessment. The new index values for 2024 and 2025 provide clear evidence that spawning biomass has increased rapidly over the preceding two years (Figure 5). It should be noted, however, that the coefficient of variation (CV) of the index values for 2025 is elevated, attributable to reduced fishing effort (Figure 6), the temporal correlation assumed in the CPUE standardization model, and delayed data submission.

2.4. Size compositions

Size composition data for bigeye tuna in purse-seine fisheries have been updated for 2024 and 2025. The mean body length of bigeye tuna caught in the OBJ fishery exhibited a rapid increase in 2025. Size composition data for bigeye tuna in longline fisheries have been updated to include 2023 and 2024, reflecting the one-year lag associated with longline data reporting. Longline observer data collected by Japan and Korea during those two years have been incorporated into this update assessment. The spatial coverage of these data has recovered from the reduced levels observed during the COVID-19 pandemic period, during which the longline observer program was severely disrupted, but is still historically low (Figure 7).

3. MODEL RESULTS

3.1. Model convergence

All thirty-six reference models examined in this update assessment have positive-definite Hessians (Table 2). A small number of reference models exhibit maximum gradients exceeding 0.01; however, they all pass the jitter diagnostics using a limited number of runs given time constraints and are therefore considered to have attained convergence in this update assessment. This issue should nonetheless be subject to further investigation in the next benchmark assessment.

3.2. Recruitment

The time series of relative annual recruitment estimates (Figure 8) exhibits several noteworthy characteristics: (1) recruitment estimates are insensitive to assumptions regarding effort creep and, in particular, steepness; (2) no pronounced regime shift in recruitment coincides with the expansion of the floating-object fishery; and (3) recruitment in 2023 is estimated as one of the highest in history, coinciding with a strong El Niño event in the Pacific Ocean.

3.3. Spawning biomass

The estimates of spawning biomass and dynamic spawning biomass ratio (SBR; the ratio of spawning biomass to unfished spawning biomass under historical recruitment) show considerable variability both within and across reference models (Figure 9). In general, these estimates demonstrate greater sensitivity to the degree of effort creep than that of steepness. This finding is anticipated, given that the longline index of abundance, which is directly influenced by the level of effort creep, represents the most important indicator of spawning biomass trend. It is worth noting that the spawning biomass trajectory displays a pronounced positive trend in 2025, likely attributable to IVT-induced reductions in juvenile fishing mortality rates since 2022 (see section 3.4). Given that the average age at maturity for bigeye in the EPO is approximately 3.5 years, and consequently, the beneficial effect of the IVT on spawning biomass would not be expected to manifest prior to 2025. Since recruitment is estimated to be markedly high in 2023, spawning biomass is projected to increase even more rapidly in 2026 and 2027 as that cohort progressively reaches maturity (SAC-17-05).

3.4. Fishing mortality (*F*)

Fishing mortality (F) for bigeye tuna in the EPO has exhibited notable fluctuations over the assessment period. Across all reference models, it is evident that F for juvenile bigeye (aged less than 9 quarters) increased substantially from near-zero levels prior to 1993 to historically high values in 2020, followed by a rapid decline attributable to the implementation of the IVT in 2022 (Figure 10a). By contrast, F for bigeye aged more than 12 quarters has remained relatively stable since 1993, with a declining trend observable from approximately 2015 onward.

4. STOCK STATUS

Two sets of target reference points are considered in this analysis: those associated with maximum sustainable yield (MSY) and those associated with 30% dynamic SBR (SAC-15-05). According to the thirty-six reference models included in this update assessment, spawning biomass at the beginning of 2026 ranges from 62% to 345% of the spawning biomass at dynamic MSY (S_{MSY_d}; derived by projecting the population into the future under historical recruitment, current fishery selectivity, and $F = F_{MSY}$) and ranges from 56% to 154% of 30% unfished dynamic spawning biomass ($S_{30\%}$; 30% unfished spawning biomass under historical recruitment) (Table 3). Average fishing mortality for 2023-2025 ranges from 28% to 90% of the fishing mortality corresponding to MSY (F_{MSY}) and ranges from 50% to 98% of the fishing mortality yielding 30% SBR ($F_{30\%}$) (Table 3).

All models in level-1 hypothesis estimate that the average fishing mortality for 2023-2025 has dropped to a level significantly below F_{MSY} and that the spawning biomass at the beginning of 2026 has increased to a level above S_{MSY_d} (Figure 10b). These interpretations are, however, subject to considerable uncertainty, as indicated by the wide confidence intervals surrounding the most recent estimate in the phase plots (Figure 11).

The joint probability distributions for both $F_{current}/F_{MSY}$ and $S_{current}/S_{MSY\_d}$ are unimodal (Figure 12). The joint cumulative distributions suggest a 0.3% probability that $F_{current}$ exceeds F_{MSY} and a 19.5% probability that $S_{current}$ falls below S_{MSY_d}. The medians of $F_{current}/F_{MSY}$ and $S_{current}/S_{MSY\_d}$ are 0.52 and 1.43, respectively (Figure 11a). The joint probability distributions for both $F_{current}/F_{30\%}$ and $S_{current}/S_{30\%}$ are also unimodal (Figure 12). The joint cumulative distributions suggest a 3.0% probability that $F_{current}$ exceeds $F_{30\%}$ and a 53.4% probability that $S_{current}$ falls below $S_{30\%}$. The medians of $F_{current}/F_{30\%}$ and $S_{current}/S_{30\%}$ are 0.70 and 0.98, respectively (Figure 11b).

Joint probability and cumulative distributions were also calculated for management quantities related to the limit reference points ($F_{current}/F_{limit}$ and $S_{current}/S_{limit}$, which corresponds to an equilibrium depletion level of 7.7%). The joint distributions suggest a 0.0% probability that $F_{current}$ exceeds F_{limit} and a 0.0% probability that $S_{current}$ falls below S_{limit}. The joint cumulative distributions suggest medians of 0.33 and 3.45 $F_{current}/F_{limit}$ and $S_{current}/S_{limit}$, respectively.

ACKNOWLEDGEMENTS

The authors gratefully acknowledge Japan for providing operational longline CPUE data through the final quarter of 2025, and Japanese scientist Takaaki Hasegawa for providing technical support that facilitated the timely production of the longline index of abundance. IATTC staff members and CPC scientists contributed valuable advice on the stock assessment, fisheries, and biology of bigeye tuna.

TABLES

TABLE 1. Fishery and "survey" fleets defined for the stock assessment of bigeye tuna in the EPO. PS = purse-seine; LL = longline; OBJ = sets on floating objects; NOA = sets on unassociated fish; DEL = sets on dolphins. See Figure 1 for area definition.
TABLA 1. Flotas pesqueras y de "estudio" definidas para la evaluación de referencia del atún patudo en el OPO. PS = cerco; LL = palangre; OBJ = lances sobre objetos flotantes; NOA = lances no asociados; DEL = lances sobre delfines. Ver la definición de las áreas en la Figura 1.

Fleet Number	Fleet type	Fleet name	Gear	Set type	Area	Catch data	Unit
1	Fishery	LL-n-A1	LL	-	1	Retained catch only	1,000s
2		LL-n-A2			2		
3		LL-n-A3			3		
4		LL-n-A4			4		
5		LL-n-A5			5		
6		LL-n-A6			6		
7		LL-n-A7			7		
8	Fishery	LL-w-A1	LL	-	1	Retained catch only	tons
9		LL-w-A2			2		
10		LL-w-A3			3		
11		LL-w-A4			4		
12		LL-w-A5			5		
13		LL-w-A6			6		
14		LL-w-A7			7		
15	Fishery	OBJ-A1	PS	OBJ	1	Retained catch + discards (inefficiency)	tons
16		OBJ-A2			2		
17		OBJ-A3			3		
18		OBJ-A4			4		
19		OBJ-A5			5		
20		OBJ-disc-EPO			1-5	Discards (size-sorting)	tons
21	Fishery	NOADEL-A1	PS	NOA+DEL	1	Retained catch + discards (all)	tons
22		NOADEL-A2			2		
23	Survey	LL-survey-EPO	LL	-	2-7	-	-

TABLE 2. The convergence table for all the reference models. Gradient is the final gradient of the assessment model, Hessian is the determinant of the Hessian matrix in log-scale, and NLL is the negative log-likelihood of the assessment model. The model definitions are provided in the text. Steepnes is the steepness of the Beverton-Holt stock-recruitment relationship.

TABLA 2. Tabla de convergencia para todos los modelos de referencia. "Gradiente" es el gradiente final del modelo de evaluación, "Hessiana" es el determinante de la matriz hessiana en escala logarítmica y "NLL" es la verosimilitud logarítmica negativa del modelo de evaluación. Las definiciones de los modelos se proporcionan en el texto. "Inclinación" es la inclinación de la relación población-reclutamiento de Beverton-Holt.

Number	Model	Catchability	Steepness	Gradient	Hessian	NLL
1	Fix	0%	1.0	0.002	648.17	1360.42
2	Fix	0%	0.9	0.004	653.03	1362.29
3	Fix	0%	0.8	0.035	655.94	1364.98
4	Fix	1%	1.0	0.023	659.28	1364.19
5	Fix	1%	0.9	0.049	660.21	1365.09
6	Fix	1%	0.8	0.005	660.65	1367.18
7	Fix	2%	1.0	0.018	662.55	1372.18
8	Fix	2%	0.9	0.000	663.76	1371.35
9	Fix	2%	0.8	0.003	663.31	1372.24
10	Gro	0%	1.0	0.004	625.64	1386.98
11	Gro	0%	0.9	0.002	627.73	1387.9
12	Gro	0%	0.8	0.025	629.82	1389.43
13	Gro	1%	1.0	0.010	632.89	1392.31
14	Gro	1%	0.9	0.001	634.30	1392.16
15	Gro	1%	0.8	0.000	633.42	1392.81
16	Gro	2%	1.0	0.000	635.88	1401.65
17	Gro	2%	0.9	0.000	635.79	1399.8
18	Gro	2%	0.8	0.010	642.43	1403.14
19	Sel	0%	1.0	0.000	652.45	1337.31
20	Sel	0%	0.9	0.002	652.67	1337.34
21	Sel	0%	0.8	0.001	652.40	1337.65
22	Sel	1%	1.0	0.006	654.52	1340.77
23	Sel	1%	0.9	0.001	656.49	1339.77
24	Sel	1%	0.8	0.010	658.95	1339.17
25	Sel	2%	1.0	0.002	658.64	1347.95
26	Sel	2%	0.9	0.003	660.98	1345.33
27	Sel	2%	0.8	0.001	662.63	1343.33
28	Mrt	0%	1.0	0.002	632.99	1350.09
29	Mrt	0%	0.9	0.004	633.88	1349.69
30	Mrt	0%	0.8	0.009	634.53	1349.63
31	Mrt	1%	1.0	0.002	600.50	1356.28
32	Mrt	1%	0.9	0.001	601.44	1354.81
33	Mrt	1%	0.8	0.000	604.60	1353.93
34	Mrt	2%	1.0	0.001	647.57	1366.29
35	Mrt	2%	0.9	0.006	649.72	1363.21

36	Mrt	2%	0.8	0.004	651.29	1361.13

TABLE 3. Management table for bigeye tuna in the EPO. $S_{current}$, S_0, S_{MSY_d}, and $S_{30\%}$: spawning biomass (metric tons) at the beginning of 2026, in an unfished equilibrium state, at dynamic MSY, and at 30% unfished dynamic state; $F_{current}$, F_{MSY}, and $F_{30\%}$: average fishing mortality between 2023-2025, at MSY, and at 30% dynamic spawning biomass ratio; S_{limit} and F_{limit}: limit reference points for spawning biomass and fishing mortality, respectively, corresponding to a equalibrium depletion level of 7.7%.

TABLA 3. Tabla de ordenación para el patudo en el OPO. S_{actual}, S_0, S_{RMS_d} y $S_{30\%}$: biomasa reproductora (toneladas métricas) al principio de 2026, en estado de equilibrio en ausencia de pesca, en RMS dinámico y en un estado dinámico en ausencia de pesca del 30%; F_{actual}, F_{RMS} y $F_{30\%}$: mortalidad por pesca promedio entre 2023-2025, en RMS y en cociente de biomasa reproductora dinámico del 30%; $S_{LÍMITE}$ y $F_{LÍMITE}$: puntos de referencia límite para biomasa reproductora y mortalidad por pesca, respectivamente, correspondientes a un nivel de reducción de equilibrio del 7.7 %.

	1	2	3	4	5	6	7	8	9
	0%-1.0	**0%-0.9**	**0%-0.8**	**1%-1.0**	**1%-0.9**	**1%-0.8**	**2%-1.0**	**2%-0.9**	**2%-0.8**
Fix									
MSY	104028	100908	99201	109406	106260	104334	115922	112888	110934
MSY_d	108300	109909	113601	106179	109205	114399	104605	109554	116827
S_0	406656	447163	500984	419814	462959	519259	437510	483986	544438
S_{MSY}/S_0	0.17	0.23	0.27	0.17	0.23	0.27	0.17	0.23	0.27
$S_{current}/S_0$	0.29	0.28	0.27	0.23	0.22	0.22	0.19	0.18	0.17
$S_{current}/S_{MSY\ d}$	1.61	1.12	0.89	1.42	0.96	0.75	1.25	0.82	0.62
$S_{current}/S_{30\%}$	0.97	0.89	0.83	0.85	0.76	0.69	0.75	0.64	0.56
$S_{current}/S_{limit}$	3.75	3.62	3.53	3.04	2.91	2.83	2.48	2.33	2.25
$F_{current}/F_{MSY}$	0.50	0.62	0.70	0.56	0.70	0.79	0.63	0.79	0.90
$F_{current}/F_{30\%}$	0.73	0.74	0.75	0.83	0.85	0.86	0.92	0.96	0.98
$F_{current}/F_{limit}$	0.50	0.62	0.70	0.56	0.70	0.79	0.63	0.79	0.90
Gro									
MSY	108744	103767	100660	114294	109147	105860	120854	115687	112912
MSY_d	112905	111425	112514	110597	109802	111931	108777	109020	112451
S_0	378133	407841	447913	392176	423738	466136	409804	443924	494136
S_{MSY}/S_0	0.17	0.23	0.27	0.17	0.23	0.27	0.17	0.23	0.27
$S_{current}/S_0$	0.32	0.31	0.30	0.27	0.25	0.25	0.22	0.21	0.20
$S_{current}/S_{MSY\ d}$	1.91	1.32	1.04	1.71	1.16	0.90	1.54	1.01	0.78
$S_{current}/S_{30\%}$	1.11	1.03	0.96	0.99	0.90	0.82	0.88	0.77	0.70
$S_{current}/S_{limit}$	4.20	4.06	3.94	3.46	3.31	3.21	2.85	2.69	2.60
$F_{current}/F_{MSY}$	0.42	0.53	0.61	0.47	0.59	0.69	0.52	0.67	0.77
$F_{current}/F_{30\%}$	0.63	0.65	0.66	0.70	0.73	0.75	0.78	0.82	0.84
$F_{current}/F_{limit}$	0.42	0.53	0.61	0.47	0.59	0.69	0.52	0.67	0.77
Sel									
MSY	122504	115627	111028	125296	118616	114308	130020	123559	119533
MSY_d	122735	118101	116092	117047	113333	112824	113048	110682	112074
S_0	522101	558274	607012	519159	557240	609609	525534	566449	623362
S_{MSY}/S_0	0.16	0.22	0.27	0.16	0.23	0.27	0.16	0.23	0.27
$S_{current}/S_0$	0.37	0.37	0.36	0.30	0.29	0.28	0.24	0.23	0.22

	1	2	3	4	5	6	7	8	9
	0%-1.0	**0%-0.9**	**0%-0.8**	**1%-1.0**	**1%-0.9**	**1%-0.8**	**2%-1.0**	**2%-0.9**	**2%-0.8**
$S_{current}/S_{MSY\_d}$	2.39	1.68	1.37	2.05	1.42	1.13	1.77	1.19	0.93
$S_{current}/S_{30\%}$	1.35	1.29	1.22	1.16	1.08	1.00	1.00	0.90	0.81
$S_{current}/S_{limit}$	4.86	4.75	4.66	3.85	3.73	3.63	3.07	2.92	2.82
$F_{current}/F_{MSY}$	0.33	0.42	0.48	0.39	0.50	0.58	0.46	0.59	0.69
$F_{current}/F_{30\%}$	0.50	0.52	0.53	0.60	0.62	0.63	0.69	0.72	0.75
$F_{current}/F_{limit}$	0.33	0.42	0.48	0.39	0.50	0.58	0.46	0.59	0.69
Mrt									
MSY	130099	119462	113353	128184	119391	114469	129337	122168	118271
MSY_d	127487	118762	115280	118036	112002	111578	111607	108783	111674
S_0	300523	318540	344023	317853	339917	371022	344492	372052	410442
S_{MSY}/S_0	0.12	0.20	0.25	0.13	0.21	0.25	0.14	0.21	0.26
$S_{current}/S_0$	0.42	0.40	0.38	0.32	0.31	0.29	0.25	0.23	0.22
$S_{current}/S_{MSY\_d}$	3.45	2.00	1.53	2.69	1.60	1.20	2.11	1.26	0.92
$S_{current}/S_{30\%}$	1.54	1.43	1.32	1.29	1.16	1.04	1.07	0.92	0.80
$S_{current}/S_{limit}$	5.46	5.23	5.00	4.20	3.97	3.77	3.24	3.01	2.83
$F_{current}/F_{MSY}$	0.28	0.40	0.48	0.36	0.50	0.60	0.44	0.61	0.73
$F_{current}/F_{30\%}$	0.50	0.52	0.55	0.62	0.65	0.68	0.74	0.78	0.82
$F_{current}/F_{limit}$	0.28	0.40	0.48	0.36	0.50	0.60	0.44	0.61	0.73

FIGURES

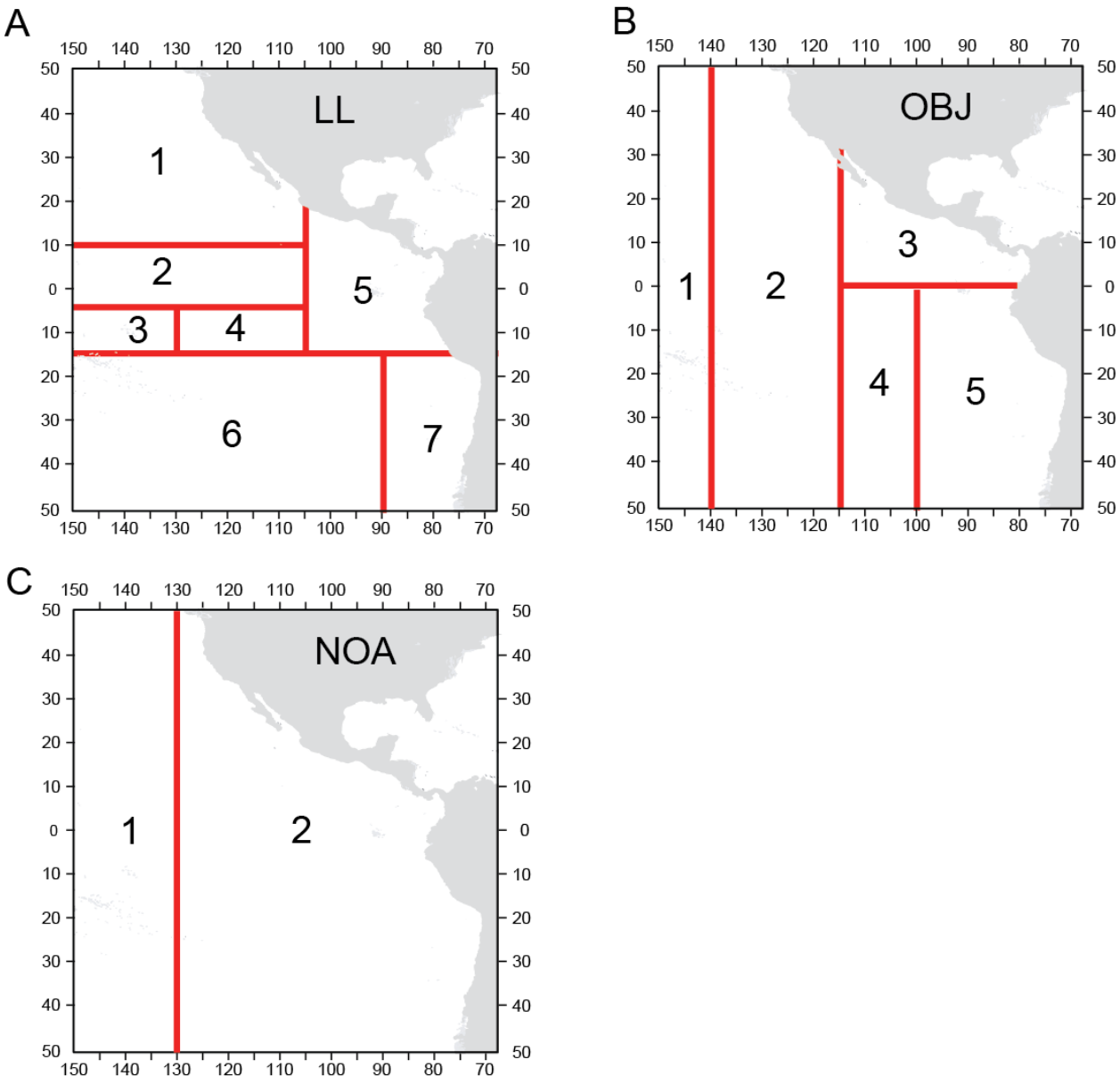

FIGURE 1. Summary of area definitions for the longline (LL), floating-object (OBJ), and unassociated (NOA) fishery fleets in the stock assessment of bigeye tuna in the EPO.

FIGURA 1. Resumen de las definiciones de áreas para las flotas de las pesquerías palangrera (LL), sobre objetos flotantes (OBJ) y no asociada (NOA) en la evaluación del atún patudo en el OPO.

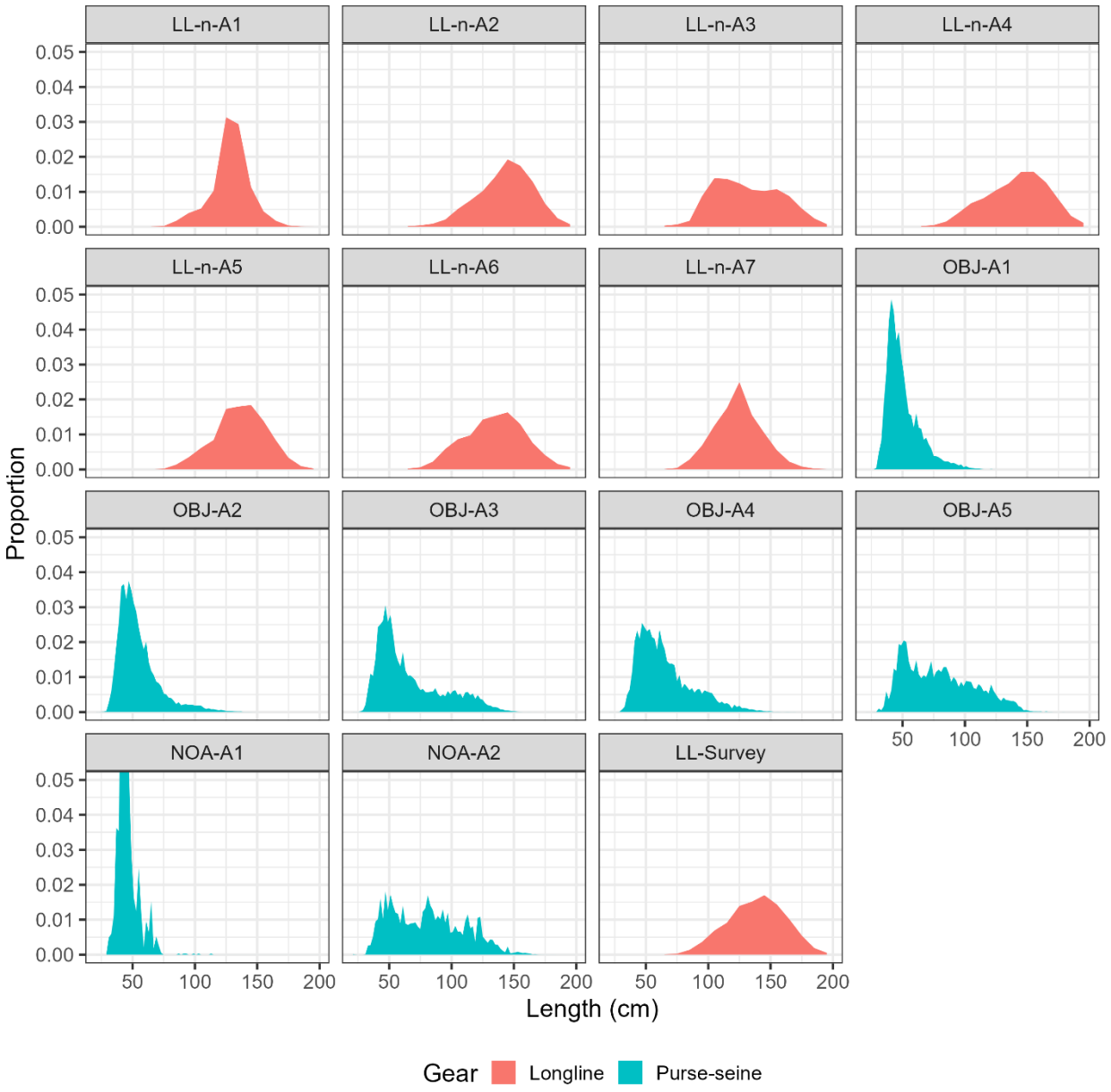

FIGURE 2. Sample-size weighted length frequency of bigeye tuna observed by each fishery and survey in the benchmark assessment model averaged over all years.
FIGURA 2. Frecuencia de talla ponderada por tamaño de muestra de atún patudo observada por cada pesquería y flota de estudio en el modelo de evaluación de referencia.

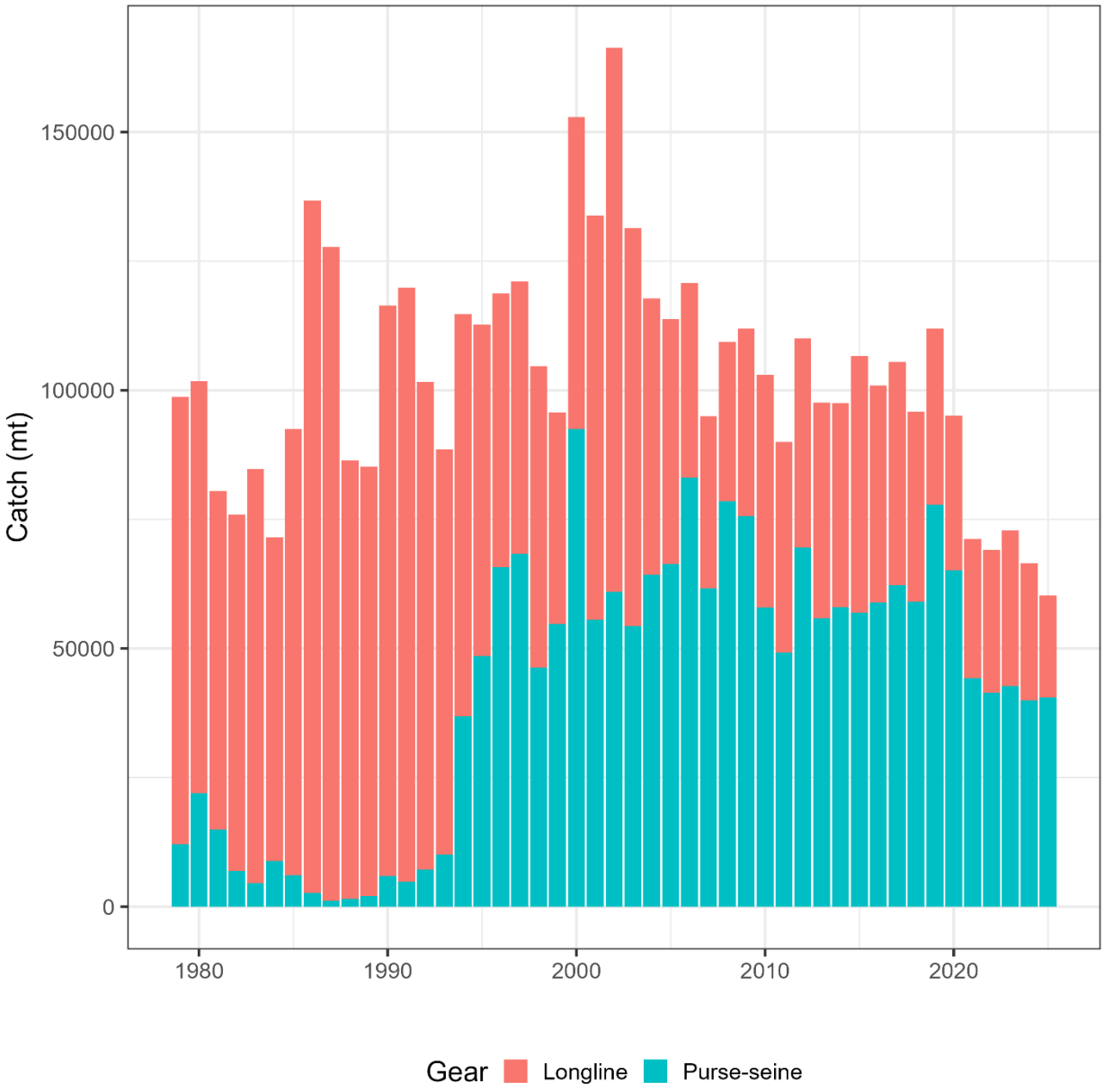

FIGURE 3. Annual catches (metric tons) of bigeye tuna in the eastern Pacific Ocean by gear type in 1979-2025.
FIGURA 3. Capturas anuales (toneladas métricas) de atún patudo en el Océano Pacífico oriental, por tipo de arte, en 1979-2025.

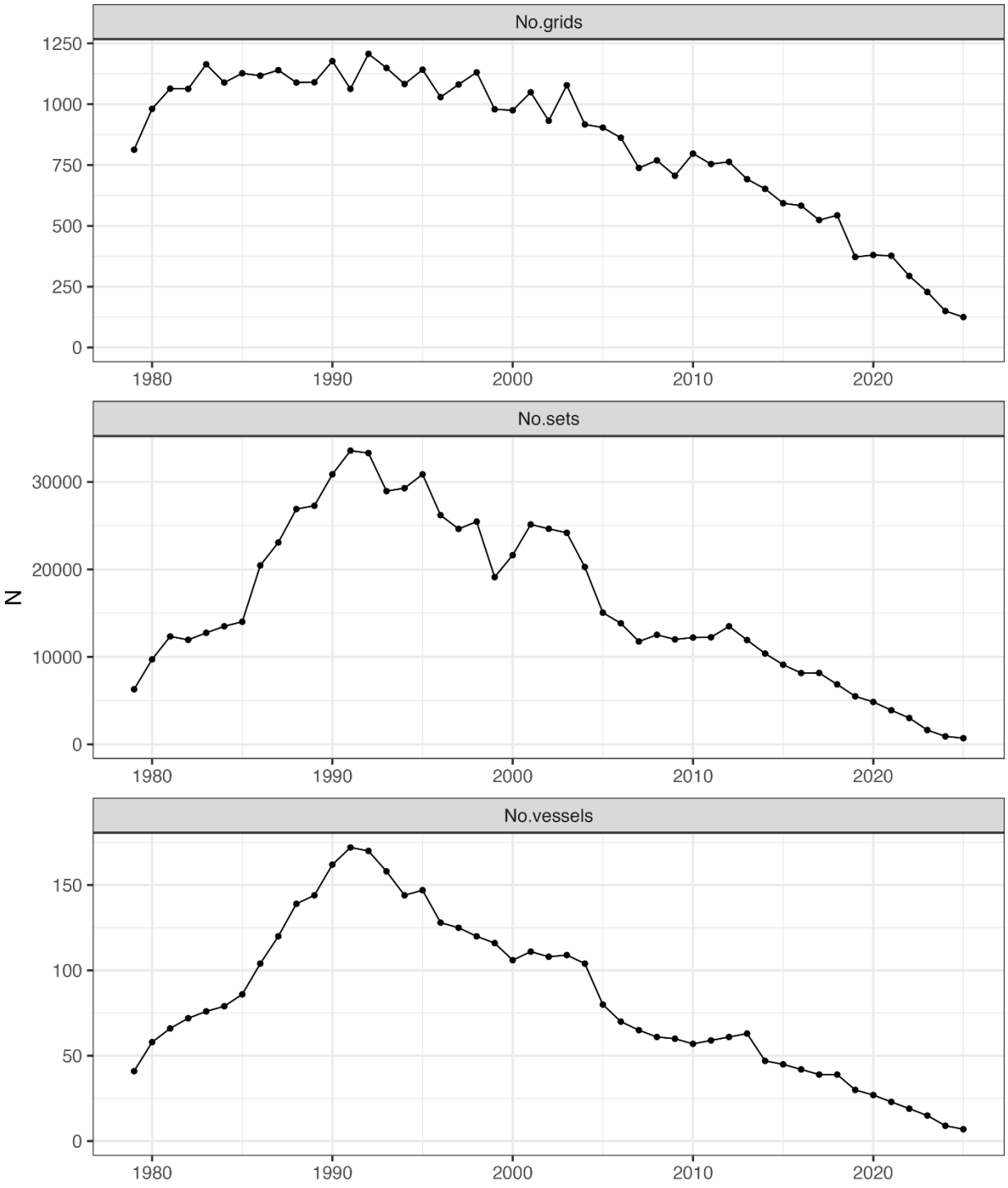

FIGURE 4. Time series of the number of 1° x 1° grid cells (top panel), sets (middle panel), and vessels (bottom panel) covered by the Japanese longline CPUE dataset between 1979 and 2025.
Figura 4. Series de tiempo del número de celdas de 1° x 1° (panel superior), lances (panel central) y buques (panel inferior) incluidos en el conjunto de datos de CPUE palangrera de Japón entre 1979 y 2025.

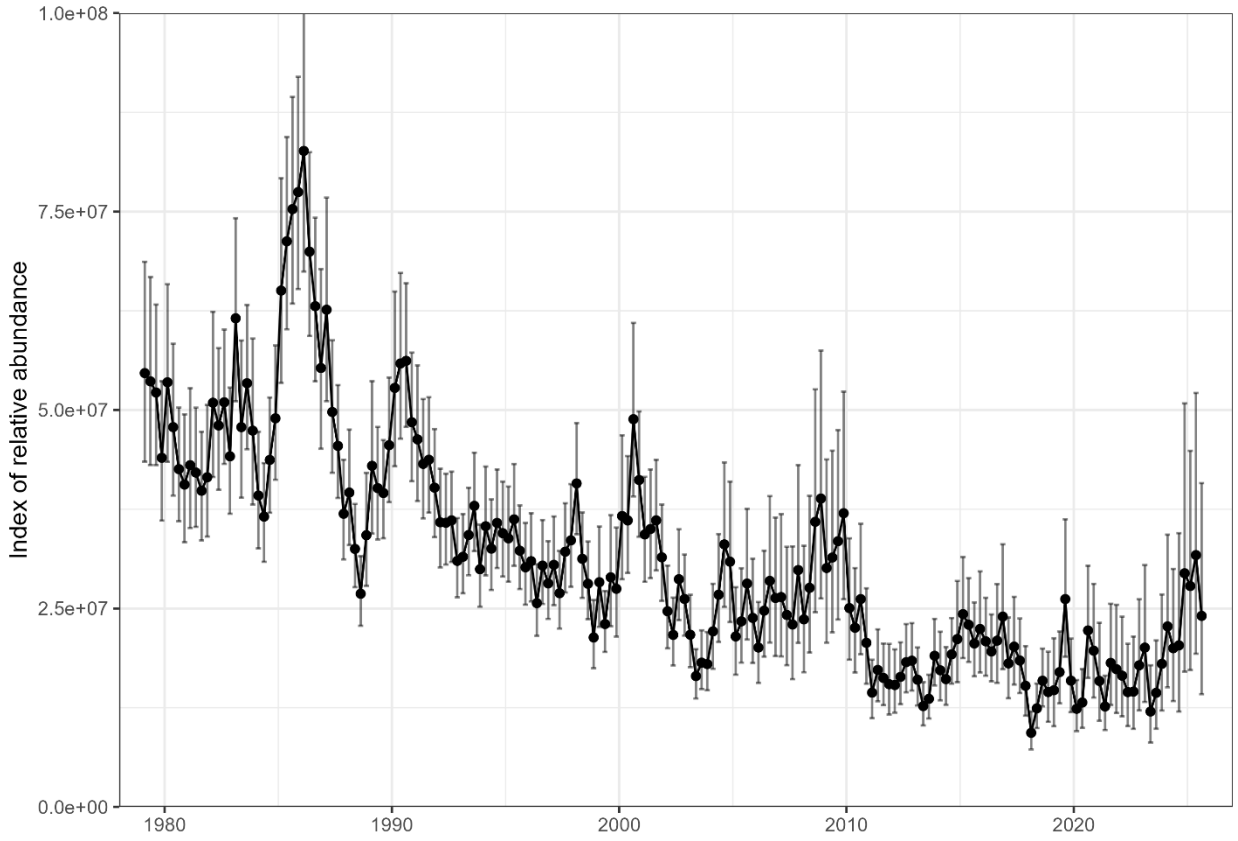

FIGURE 5. The standardized longline index of abundance and its 95% confidence interval estimated by the spatiotemporal model for bigeye tuna.
FIGURA 5. Índice estandarizado de abundancia y su coeficiente de variación del 95% estimados por el modelo espaciotemporal para el atún patudo.

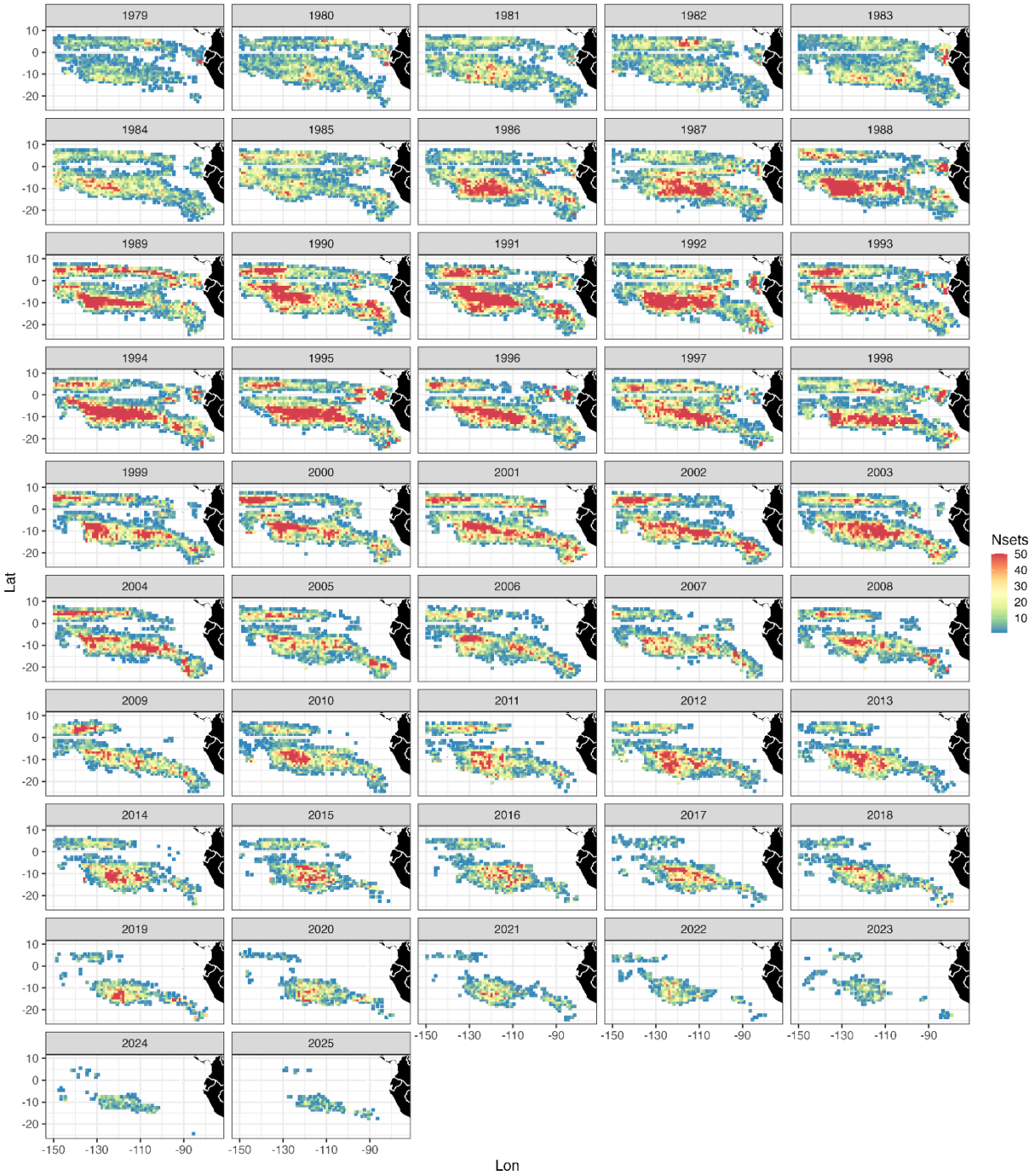

FIGURE 6. Spatial distribution of the annual number of sets made by the Japanese longline fleet operating in the eastern Pacific Ocean between 1979 and 2025.

FIGURA 6. Distribución espacial del número anual de lances de la flota palangrera de Japón en el Océano Pacífico oriental entre 1979 y 2025.

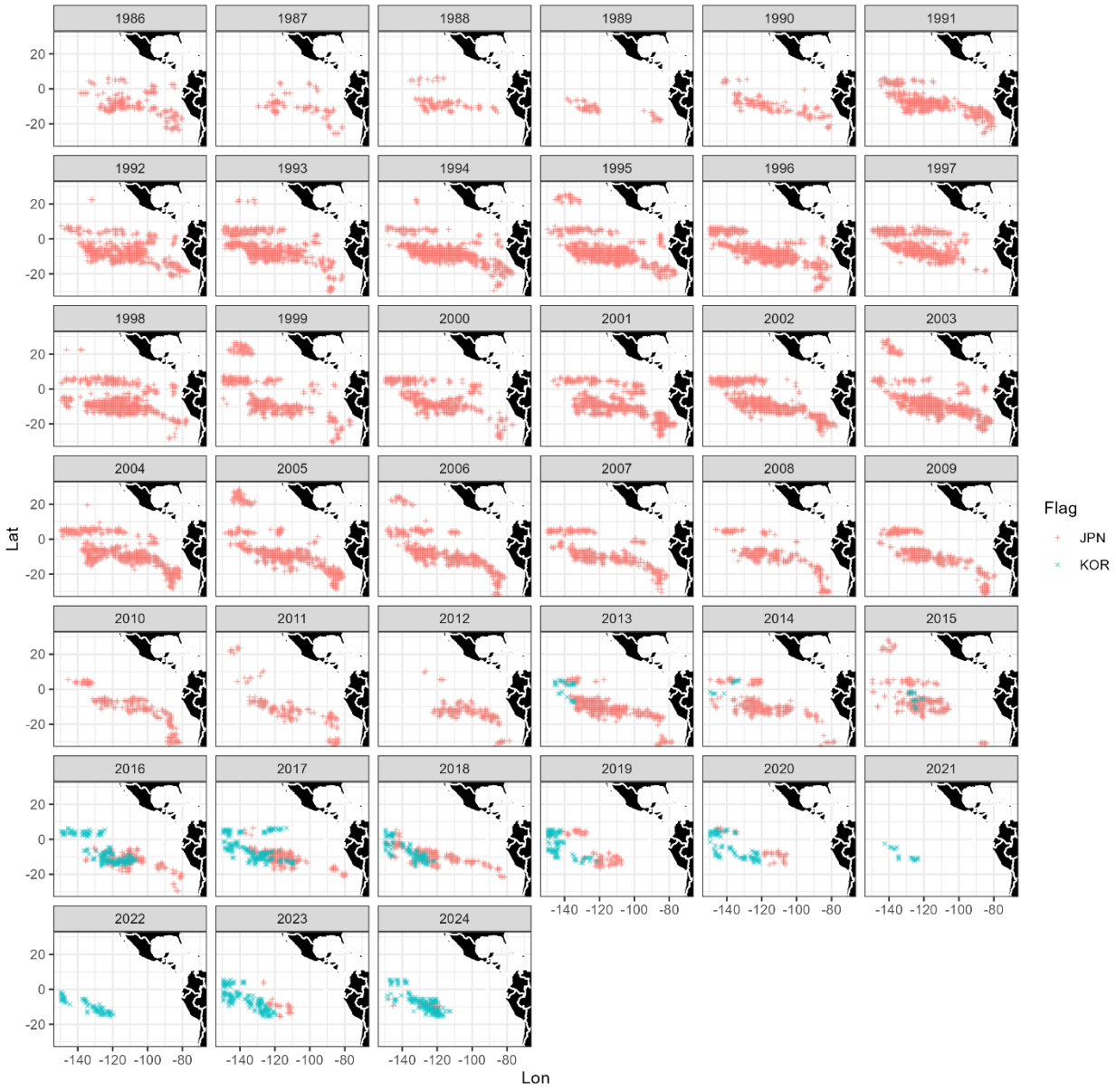

FIGURE 7. The spatiotemporal distribution of the Japanese and Korean longline length composition data used in this update assessment. The composition data comes from fishers and observers. Data only comes from observers after 2020.

FIGURA 7. Distribución espaciotemporal de los datos de composición por talla de palangre de Japón y Corea utilizados en esta evaluación actualizada. Los datos de composición proceden de pescadores y observadores. A partir de 2020, los datos proceden solo de observadores.

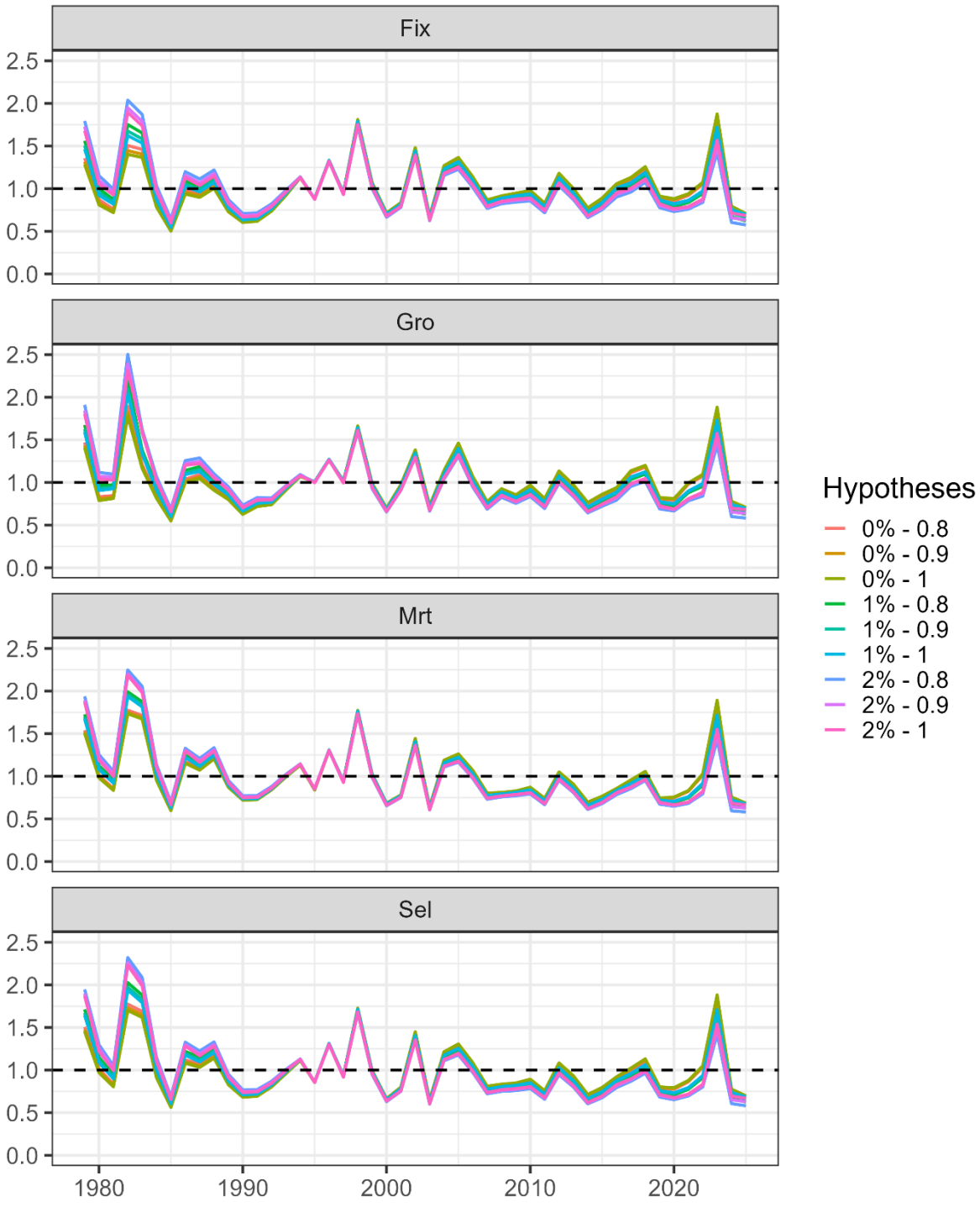

FIGURE 8. Comparison of estimated relative annual recruitment of bigeye tuna between 1979 and 2025.
FIGURA 8. Comparación del reclutamiento anual relativo estimado del atún patudo entre 1979 y 2025.

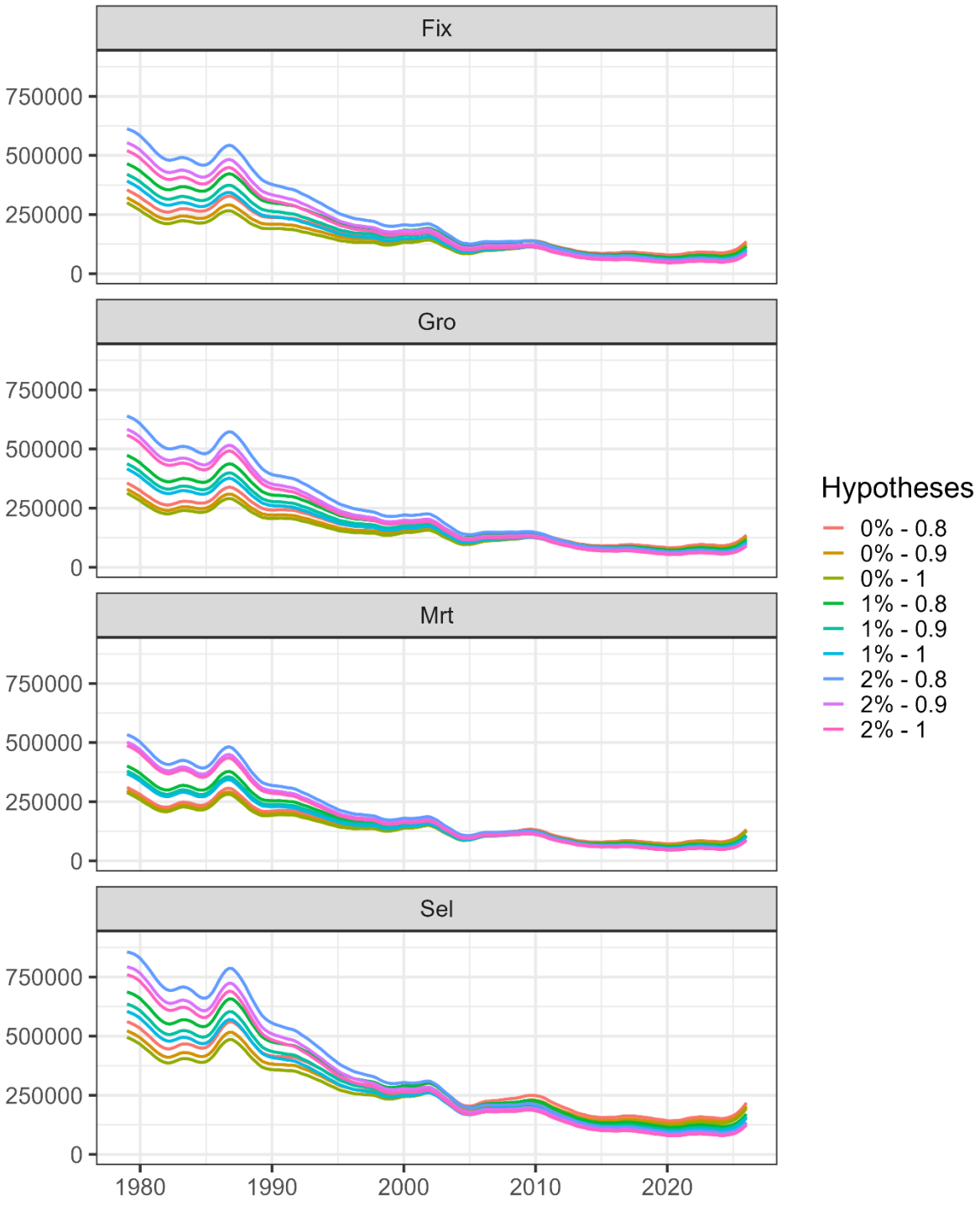

FIGURE 9a. Comparison of estimated spawning biomass of bigeye tuna between 1979 and 2025.
FIGURA 9a. Comparación de la biomasa reproductora estimada del atún patudo entre 1979 y 2025.

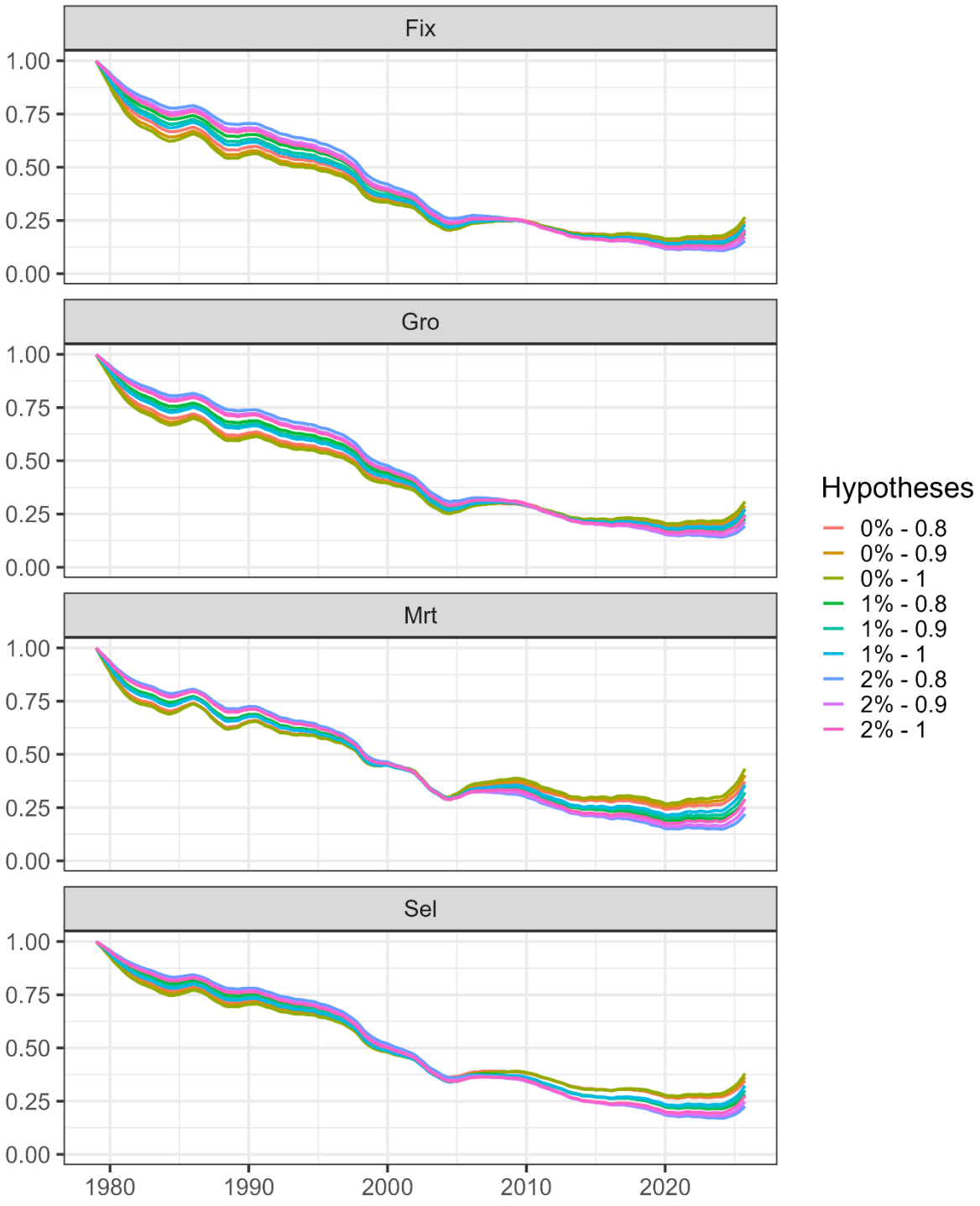

FIGURE 9b. Comparison of estimated dynamic spawning biomass ratio of bigeye tuna between 1979 and 2025.

FIGURA 9b. Comparación del cociente de biomasa reproductora del atún patudo entre 1979 y 2025.

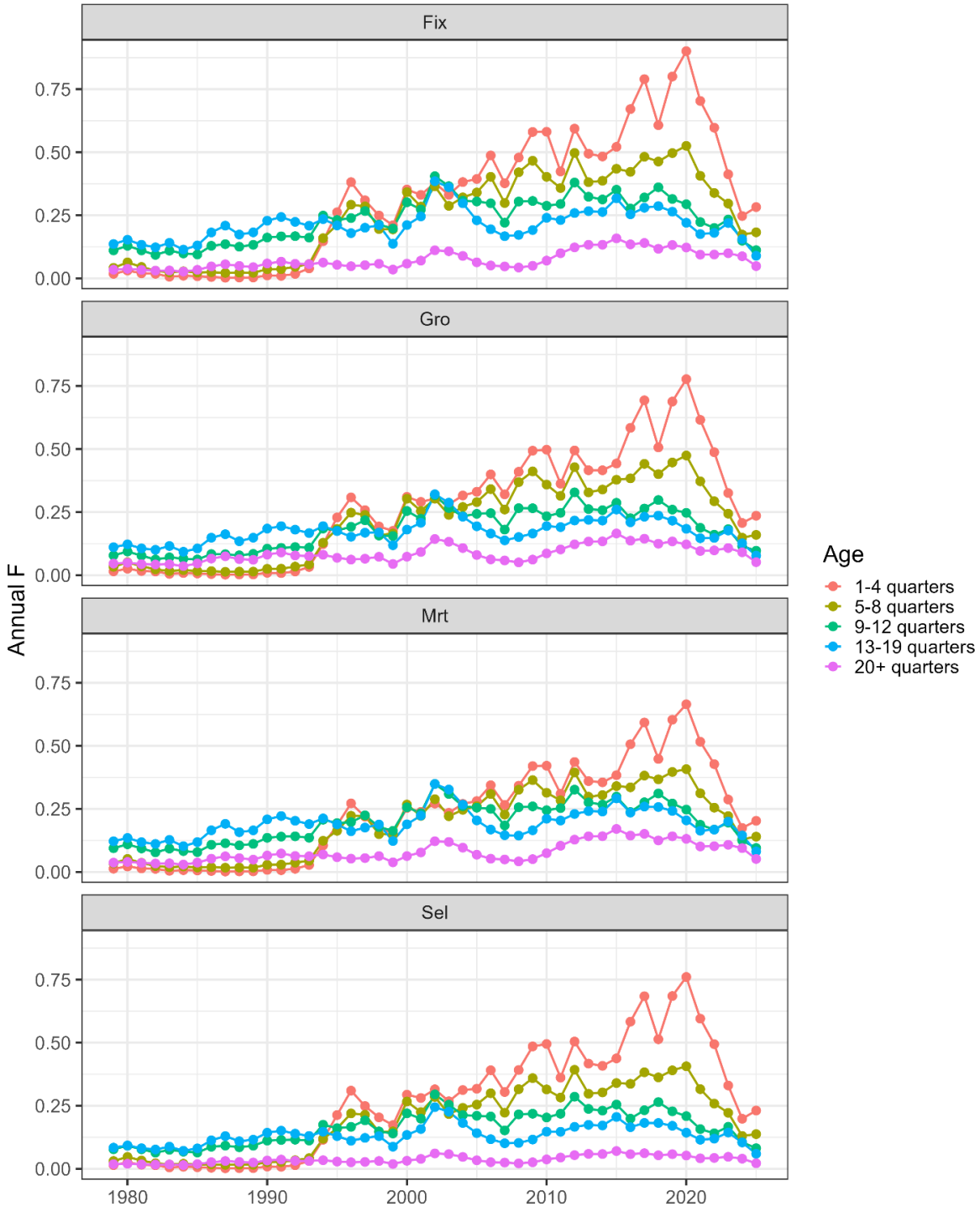

FIGURE 10a. Comparison of average annual fishing mortality, by age groups, of bigeye tuna between 1979 and 2025. The values for each model and age group are the weighted average across the second- and third-level hypotheses.

FIGURA 10a. Comparación de la mortalidad por pesca anual promedio, por grupos de edad, del atún patudo entre 1979 y 2025. Los valores de cada modelo y grupo de edad son el promedio ponderado de las hipótesis de segundo y tercer nivel.

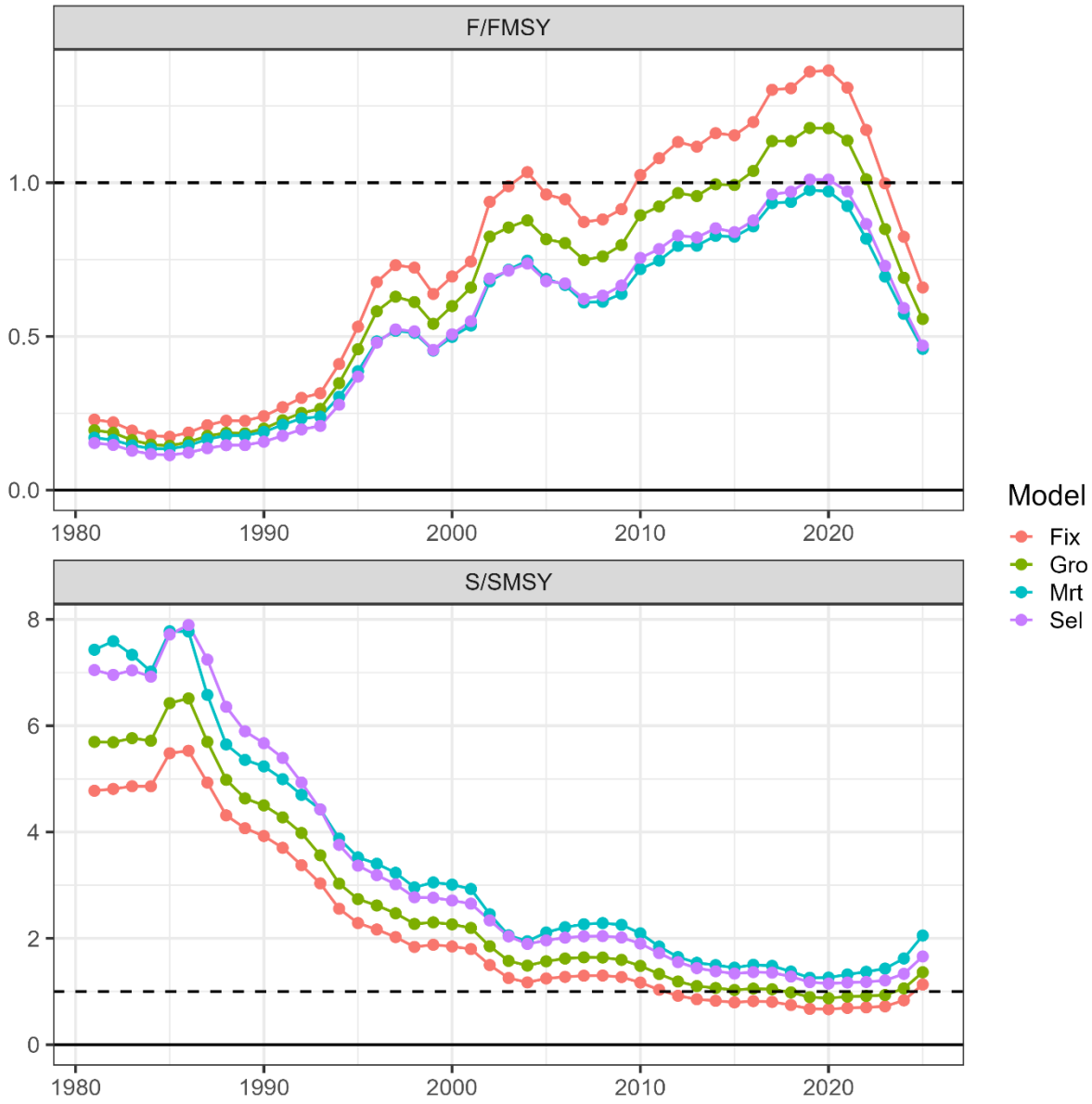

FIGURE 10b. Time series of estimated spawning biomass (S) and fishing mortality (F) relative to their MSY reference points for the four models considered in the level 1 hypothesis. The values for each model are weighted across the second- and third-level hypotheses, and each F is based on the average value over three years.

FIGURA 10b. Series de tiempo de la biomasa reproductora (*S*) y la mortalidad por pesca (*F*) estimadas en relación con sus puntos de referencia de RMS para los cuatro modelos considerados en la hipótesis de nivel 1. Los valores de cada modelo se ponderan entre las hipótesis de segundo y tercer nivel, y cada F se basa en el valor promedio de tres años.

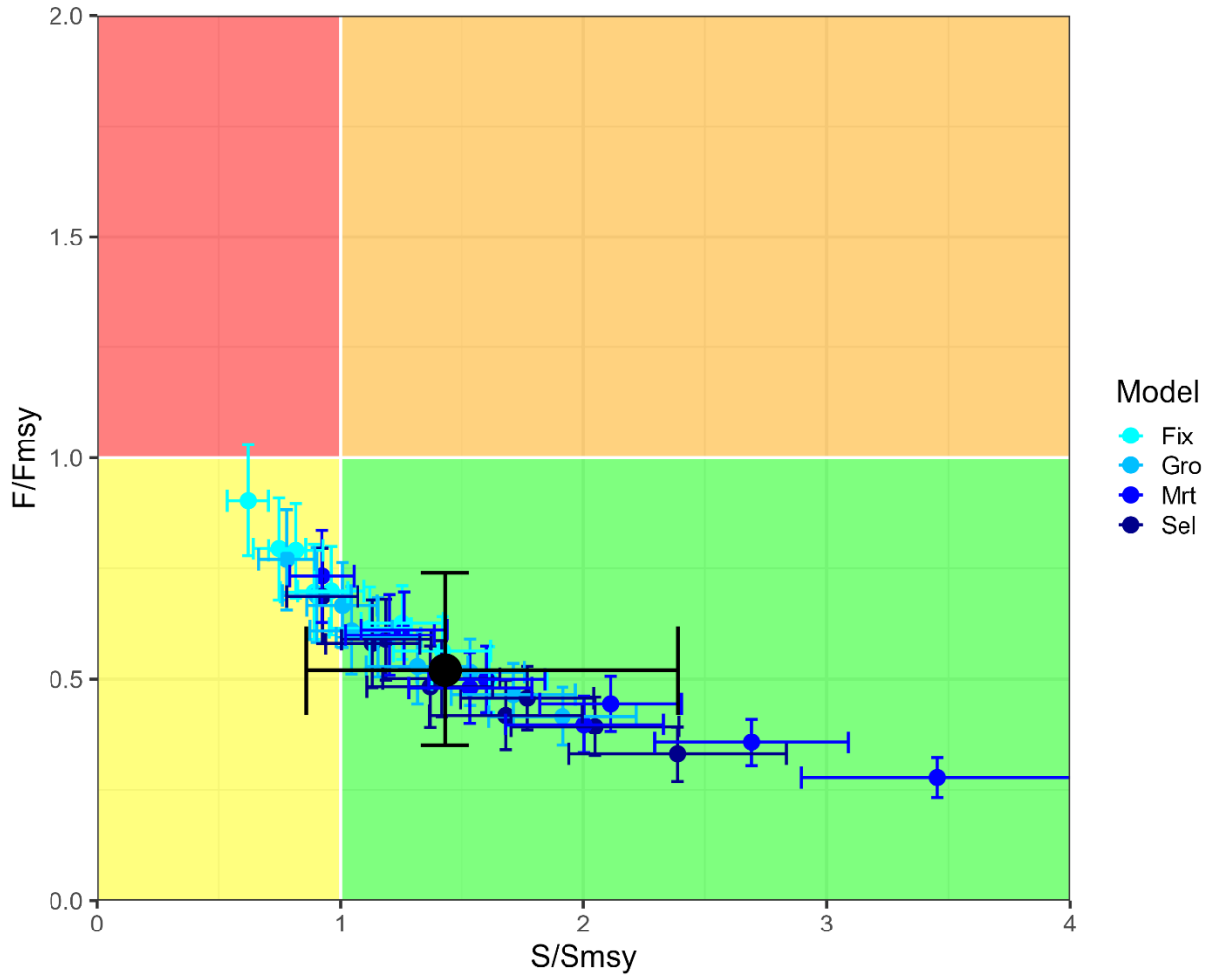

FIGURE 11A. Phase (Kobe) plot of the most recent estimates of spawning biomass (*S*) and fishing mortality (*F*) relative to their MSY reference points (S_{MSY_d} and F_{MSY}) from the thirty-six reference models. Each color dot is based on *S* at the beginning of 2026 and average *F* over the most recent three years, 2023-2025, and its error bars represent the 80% confidence interval of model estimates. The large black circle and error bars represent the median and 80% confidence interval combined over all models, respectively.

FIGURA 11a. Gráfica de fase (Kobe) de las estimaciones más recientes de la biomasa reproductora (*S*) y la mortalidad por pesca (*F*) en relación con sus puntos de referencia de RMS (S_{RMS_d} and F_{RMS}) a partir de los 36 modelos de referencia. Cada punto de color se basa en *S* a principios de 2026 y el promedio de *F* durante los tres últimos años, 2023-2025, y sus barras de error representan el intervalo de confianza del 80% de las estimaciones de los modelos. El círculo negro grande y las barras de error representan la mediana y el intervalo de confianza del 80% combinados para todos los modelos, respectivamente.

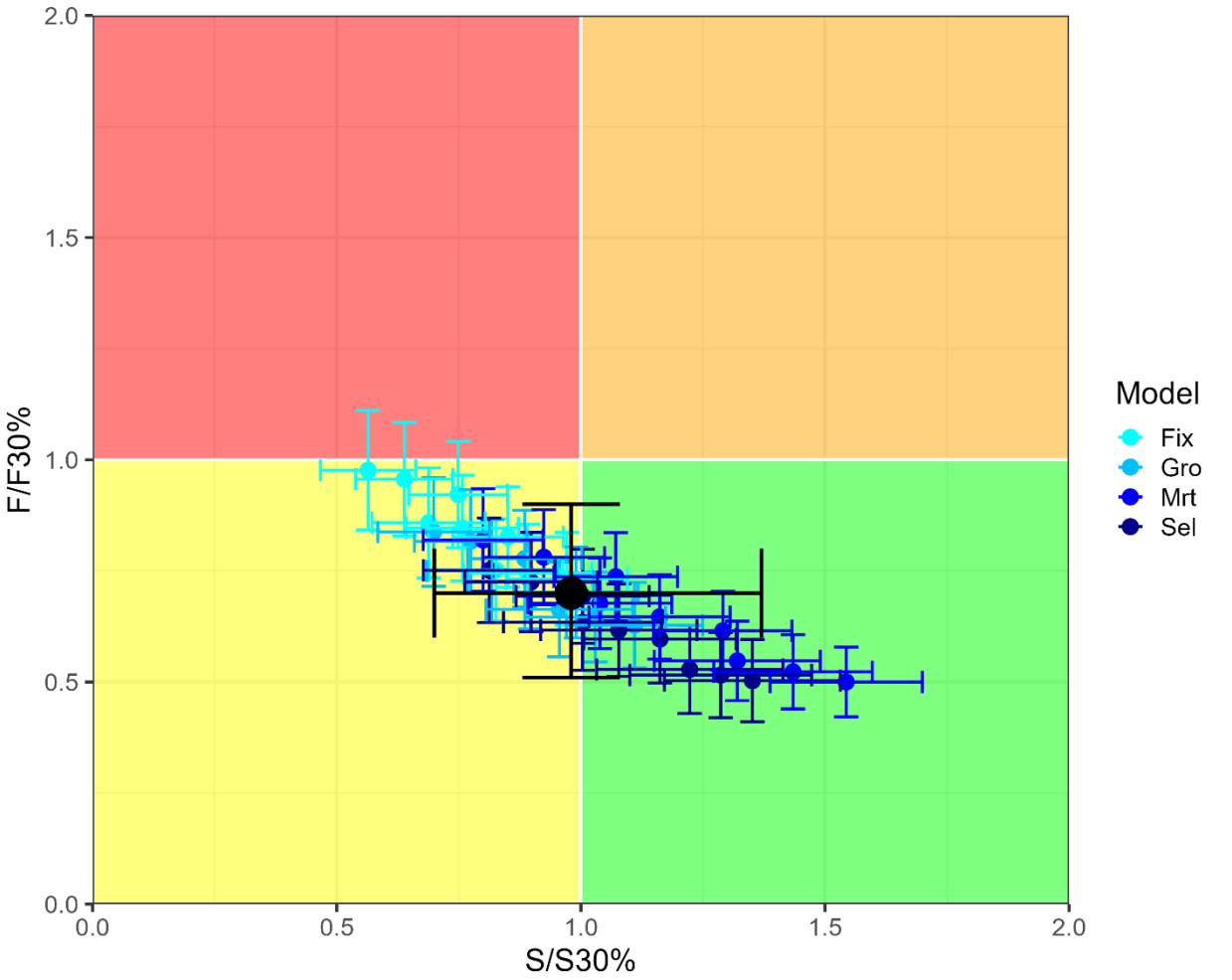

FIGURE 11B. Phase plot of the most recent estimates of spawning biomass (*S*) and fishing mortality (*F*) relative to their 30% dynamic SBR reference points ($S_{30\%}$ and $F_{30\%}$) from the thirty-six reference models. Each color dot is based on *S* at the beginning of 2026 and average *F* over the most recent three years, 2023-2025, and its error bars represent the 80% confidence interval of model estimates. The large black circle and error bars represent the median and 80% confidence interval of combined over all models, respectively.

FIGURA 11B. Gráfica de fase de las estimaciones más recientes de la biomasa reproductora (S) y la mortalidad por pesca (F) en relación con sus puntos de referencia de SBR dinámico del 30% ($S_{30\%}$ y $F_{30\%}$) a partir de los 36 modelos de referencia. Cada punto de color se basa en *S* a principios de 2026 y el promedio de *F* durante los tres últimos años, 2023-2025, y sus barras de error representan el intervalo de confianza del 80% de las estimaciones de los modelos. El círculo negro grande y las barras de error representan la mediana y el intervalo de confianza del 80% combinados para todos los modelos, respectivamente.

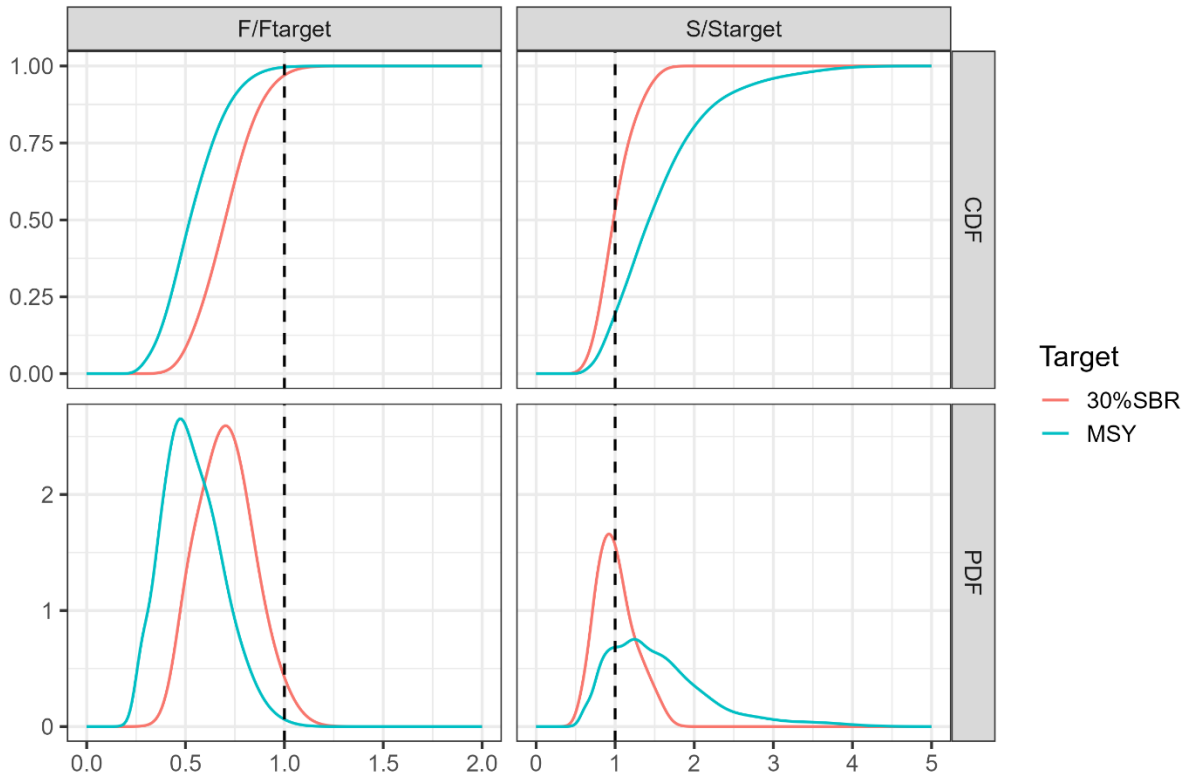

FIGURE 12. The joint probability and cumulative distributions for spawning biomass (S) in the first quarter of 2026 and fishing mortality (F) averaged over 2023-2025 relative to their MSY reference points (S_{MSY_d} and F_{MSY}).

FIGURA 12. Distribuciones conjuntas de probabilidad y acumulativas de la biomasa reproductora (*S*) en el primer trimestre de 2026 y de la mortalidad por pesca (*F*) promediada entre 2023 y 2025, en relación con sus puntos de referencia de RMS (S_{RMS_d} and F_{RMS}).

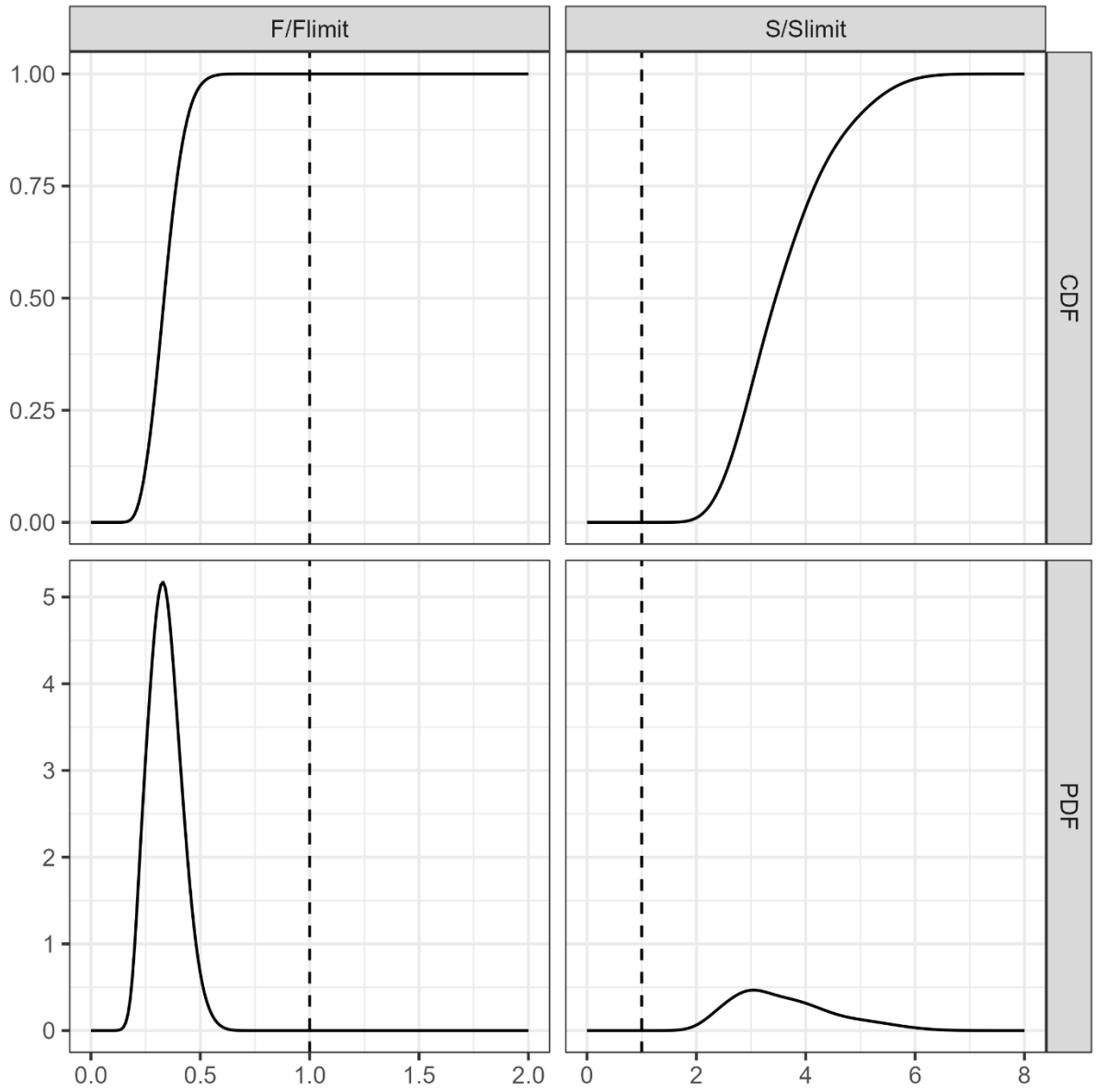

FIGURE 13. The joint probability and cumulative distributions for spawning biomass (S) in the first quarter of 2026 and fishing mortality (F) averaged over 2023-2025 relative to their limit reference points (S_{Limit} and F_{Limit}).

FIGURA 13. Distribuciones conjuntas de probabilidad y acumulativas de la biomasa reproductora (*S*) en el primer trimestre de 2026 y de la mortalidad por pesca (*F*) promediada entre 2023 y 2025, en relación con sus puntos de referencia límite ($S_{Límite}$ and $F_{Límite}$).